

## PAPER

[View Article Online](#)  
[View Journal](#) | [View Issue](#)Cite this: *Dalton Trans.*, 2020, **49**, 5703**Oxaliplatin and [Pt(*R,R*-DACH)(panobinostat-<sub>2H</sub>)] show nanomolar cytotoxicity towards diffuse intrinsic pontine glioma (DIPG)†**Marie H. C. Boulet,<sup>a</sup> Laura K. Marsh,<sup>a</sup> Alison Howarth,<sup>b</sup> Alice Woolman<sup>a</sup> and Nicola J. Farrer<sup>id</sup> <sup>✉</sup>

We report the synthesis of two novel platinum(II) complexes which incorporate histone deacetylase (HDAC) inhibitors: [Pt<sup>II</sup>(*R,R*-DACH)(Sub-<sub>H</sub>)] (**1**), [Pt<sup>II</sup>(*R,R*-DACH)(panobinostat-<sub>2H</sub>)] (**2**), where Sub<sub>H</sub> = suberoyl-bis-hydroxamic acid; DACH = (1*R*,2*R*)-(–)-1,2-diaminocyclohexane and panobinostat = (*E*)-*N*-hydroxy-3-[4-[[2-(2-methyl-1*H*-indol-3-yl)ethylamino]methyl]phenyl]prop-2-enamide. Complexes **1** and **2** were characterised by <sup>1</sup>H, <sup>13</sup>C, <sup>195</sup>Pt NMR spectroscopy and ESI-MS. Whilst oxaliplatin demonstrated considerable cytotoxicity in two patient-derived low-passage paediatric glioma DIPG cell lines (IC<sub>50</sub> values of 0.333 μM in SU-DIPG-IV, and 0.135 μM in SU-DIPG-XXI), complex **2** showed even greater cytotoxicities, with IC<sub>50</sub> values of 0.021 μM (SU-DIPG-IV), 0.067 μM (BIOMEDE 194) and 0.009 μM (SU-DIPG-XXI). Complex **2** also demonstrated superior aqueous solubility in comparison to panobinostat. Complex **2** released free intact panobinostat under HPLC conditions, as determined by ESI-MS. Incubation of solutions of oxaliplatin (H<sub>2</sub>O) and panobinostat (DMF) resulted in instantaneous reactivity and precipitation of a panobinostat derivative which was not a platinum complex; the same reactivity was not observed between carboplatin and panobinostat.

Received 23rd December 2019,  
Accepted 26th March 2020

DOI: 10.1039/c9dt04862f

[rsc.li/dalton](http://rsc.li/dalton)**Introduction**

Brain tumours are the most common cause of cancer-related death for children and young people under 40.<sup>1</sup> Diffuse midline glioma, H3 K27M-mutant (previously known as diffuse intrinsic pontine glioma (DIPG)) is highly aggressive, with a poor clinical prognosis, such that it is the leading cause of death from brain cancer in children.<sup>2</sup> Surgical removal is not possible for DIPG, due to the brainstem location and diffuse tumour nature. Radiotherapy can be mildly effective in 70% of cases – prolonging survival by up to 6 months, after which period the tumour grows back, leading to death; the 5-year survival rate for DIPG is just 1%.<sup>2</sup>

A key challenge for the therapeutic treatment of DIPG is the delivery of agents across the typically intact blood brain barrier (BBB).<sup>3</sup> Combined therapies such as carboplatin and the histone deacetylase (HDAC) inhibitor sodium valproate are reportedly synergistic towards DIPG *in cellulo*<sup>4</sup> and direct delivery of these agents to the brainstem by convection-enhanced

delivery (CED) is used clinically.<sup>5</sup> DIPG cell lines<sup>6</sup> and xenograft models<sup>6,7</sup> also demonstrate sensitivity to the potent broad-spectrum HDAC inhibitor panobinostat (Fig. 1),<sup>8</sup> and panobinostat is being evaluated in several clinical trials for DIPG (e.g. NCT02717455, NCT03632317 and NCT03566199). CED delivery of panobinostat itself,<sup>6</sup> a micellar formulation of panobinostat,<sup>9</sup> and a PET-reporting <sup>18</sup>F-panobinostat derivative<sup>10</sup> *in vivo* have also been reported. Panobinostat is only sparingly soluble in aqueous media, and initiatives to increase the solubility and cellular delivery are highly desirable. Co-ordination of bioactive ligands to platinum drugs is an established strategy, which can improve solubility, also having the potential to result in a synergistic anti-cancer effect, since the

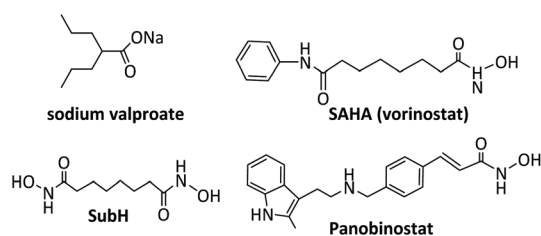


**Fig. 1** Structures of common histone deacetylase (HDAC) inhibitors in widespread use.

<sup>a</sup>Chemistry Research Laboratory, University of Oxford, 12 Mansfield Road, Oxford, OX1 3TA, UK. E-mail: Nicola.Farrer@chem.ox.ac.uk; Tel: +44 (0)1865 285131

<sup>b</sup>Structural Genomics Consortium, University of Oxford, Oxford, UK

† Electronic supplementary information (ESI) available: Synthetic details, characterisation data and cytotoxicity data. See DOI: 10.1039/c9dt04862f

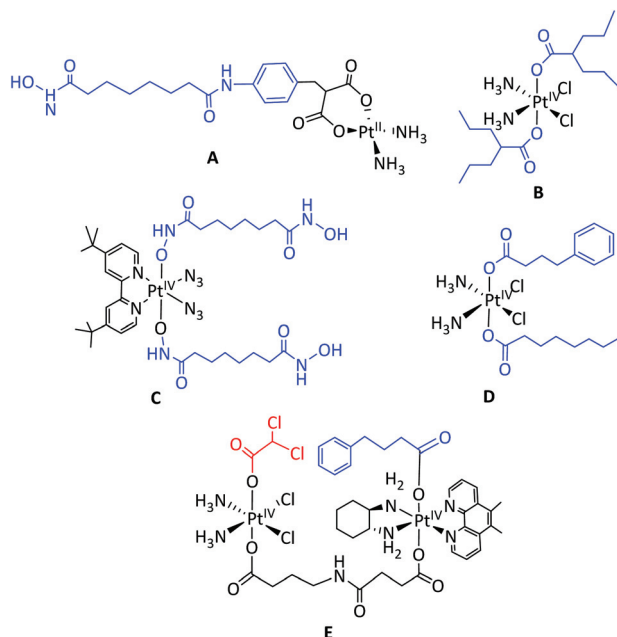


**Fig. 2** Pt HDAC inhibitor complexes. **A:**  $\text{cis-}[\text{Pt}^{\text{II}}(\text{NH}_3)_2(\text{malSAHA-2H})]$  (where SAHA = suberoylanilide hydroxamic acid),<sup>25,26</sup> **B:**  $\text{Pt}^{\text{IV}}$  valproate complex;<sup>27–29</sup> **C:**  $\text{Pt}^{\text{IV}}$  Sub complex; **D:**  $\text{cis,trans,cis-}[\text{Pt}(\text{NH}_3)_2(\text{OA})(\text{PhB})\text{Cl}_2]$  where OA = octanoate and PhB = phenylbutyrate.<sup>30</sup> **E** = dinuclear  $\text{Pt}^{\text{IV}}$  multi-modal complex. HDAC inhibitors are labelled in blue, kinase inhibitors (DCA) in red.<sup>15</sup>

platinum fragment and bioactive ligand typically exert anti-cancer activity through different mechanisms.<sup>11–14</sup> Several types of therapeutics have been coordinated to platinum complexes, including kinase inhibitors<sup>15</sup> anti-inflammatories,<sup>16</sup> and HDAC inhibitors (see Fig. 2). Several HDAC inhibitors (*e.g.* SubH, panobinostat) contain a hydroxamic acid group which chelates  $\text{Zn}^{2+}$  in the active site of certain HDAC enzymes; any HDAC delivery agent must therefore preserve the integrity of the hydroxamic functional group.<sup>17,18</sup>

For these hydroxamic acid HDAC inhibitors, the central region of the molecule occupies the histone deacetylase enzyme's narrow channel, and the terminal group interacts with residues on the enzyme surface. Histone deacetylase inhibition can lead to increased global acetylation levels and relaxation of nuclear DNA, followed by modification of gene regulation and protein recruitment. The precise mechanisms of anti-cancer activity of a given HDAC inhibitor is both cancer-specific and relatively complex.<sup>19,20</sup>

Established platinum(II) anti-cancer complexes exert their anti-cancer effect primarily by cross-linking DNA (*e.g.* cisplatin, carboplatin)<sup>21</sup> or through alternative mechanisms such as the induction of ribosomal biogenesis stress (*e.g.* oxaliplatin).<sup>22</sup> Oxaliplatin has also been shown to induce multi-faceted biological effects in murine glioma cells at sub-apoptotic drug concentrations.<sup>23</sup> Once a platinum(II) compound is taken up into a cancer cell, the chelating spectator ligands (cyclobutane-1,1-dicarboxylate and oxalate, for carboplatin and oxaliplatin respectively) dissociate. For oxaliplatin, it is the oxalate ligand,

rather than the aquated  $\text{Pt}^{\text{II}}\text{-1R,2R}$ -diamminocyclohexane species which is implicated in the common treatment side-effect; peripheral sensory neuropathy (nerve damage).<sup>24</sup>

Both platinum-based drugs and hydroxamic acid-based HDAC inhibitors are in widespread clinical use for chemotherapy. The hydroxamic acid HDAC inhibitor vorinostat has previously been combined with cisplatin (NCT01045538, NCT00867178, NCT00106626) or carboplatin<sup>31,32</sup> for a number of indications *in cellulo* and in clinical trials.<sup>33</sup> Synergies have been reported when using vorinostat and oxaliplatin for hepatocellular carcinoma *in vitro* and *in vivo*.<sup>34</sup> Several reports have detailed the coordination and co-delivery of hydroxamic acids with platinum(II) complexes,<sup>35</sup> for either their HDAC inhibitory or NO releasing properties.<sup>36</sup> Notably, the hydroxamic acid suberoylanilide hydroxamic acid (SAHA) was derivatised with malonate (malSAHA) at the terminal end, with (carboplatin-like) platinum(II) coordination through the malonate group rather than the hydroxamic acid (complex **A**, Fig. 2). Although this enabled successful platinum(II) coordination, the resulting complex exhibited no HDAC inhibitory activity in the cell line tested.<sup>25,26</sup> Our preliminary cytotoxicity data (Table 1) indicated that oxaliplatin showed promising cytotoxicity – significantly higher than carboplatin – towards DIPG cell lines. We were therefore keen to evaluate the effect of combining both oxaliplatin and structural derivatives of oxaliplatin with additional therapeutics. Different strategies for incorporating the hydroxamic acid HDAC inhibitors SubH and panobinostat within the coordination sphere of platinum were investigated, including the replacement of the oxalate ligand of oxaliplatin. We characterised the resultant novel platinum complexes and compared their biological activity to that of established chemotherapeutics, and report our findings here.

## Results and discussion

### Synthesis and characterisation of novel platinum(II) complexes

Oxaliplatin was purchased from MedChemTronica and used as received (purity data in ESI†);  $[\text{Pt}^{\text{II}}(\text{R,R-DACH})\text{Cl}_2]$ <sup>37</sup> was synthesised by literature methods (see ESI†). Treatment of  $[\text{Pt}^{\text{II}}(\text{R,R-DACH})\text{Cl}_2]$  with  $\text{AgNO}_3$  in  $\text{H}_2\text{O}$  abstracted the chloride ligands, with  $\text{AgCl}$  removed by filtration. Following addition of the hydroxamic acid (SubH or panobinostat), the solution was stirred and then concentrated under reduced pressure. The compounds  $[\text{Pt}^{\text{II}}(\text{R,R-DACH})(\text{Sub-H})]$  [**1**] and  $[\text{Pt}^{\text{II}}(\text{R,R-DACH})(\text{panobinostat-2H})]$  [**2**] were isolated by mass-directed prep-HPLC ( $\text{MeCN} + 0.1\% \text{NH}_4\text{OH}/\text{H}_2\text{O} + 0.1\% \text{NH}_4\text{OH}$ , pH 9) and lyophilised (Fig. 3). Complex **1** demonstrated good aqueous solubility (maximum solubility  $344 \text{ mg mL}^{-1}$ ,  $672 \text{ mM}$ ), as determined by ICP-MS. Complex **2** was sparingly soluble in  $\text{H}_2\text{O}$  (maximum solubility  $0.047 \text{ mg mL}^{-1}$ ,  $0.072 \text{ mM}$ ), but to a greater extent than free panobinostat (maximum aqueous solubility:  $0.000834 \text{ mg mL}^{-1}$  (calculation – ALOGPS);  $20 \text{ }\mu\text{M}$ – $50 \text{ }\mu\text{M}$  (experimentally reported)). Complex **2** showed good solubility in *d*-DMF ( $49 \text{ mg mL}^{-1}$ ,  $74 \text{ mM}$ ). Complexes **1** and **2** were characterised by HRMS, NMR spectroscopy ( $^1\text{H}$ ,  $^{13}\text{C}$ ,



**Table 1** Cytotoxicity screening data (IC<sub>50</sub>) for established and novel compounds in three different DIPG cell lines

Compound	Diffuse intrinsic pontine glioma (DIPG) cell line					
	SU-DIPG-IV		BIOMEDE 194		SU-DIPG-XXI	
	IC <sub>50</sub> (μM)	95% CI (μM)	IC <sub>50</sub> (μM)	95% CI (μM)	IC <sub>50</sub> (μM)	95% CI (μM)
Carboplatin	66.3	30–143	78.5 <sup>b</sup>	55–133	>5	—
Oxaliplatin	0.333	0.108–1.043	>5	—	0.135	0.101–0.179
SubH	210.7 <sup>a</sup>	123.1–370.7	>5	—	>5	—
Panobinostat	0.002	0.002–0.003	0.027	0.015–0.049	0.002	0.001–0.002
1 : 1 Oxaliplatin + Panobinostat	0.006	0.004–0.009	0.023	0.0153–0.034	0.003	0.002–0.004
1 : 1 Oxaliplatin + SubH	0.552	0.226.7–1.504	>5	—	0.250	0.177–0.354
Complex 1	>5	—	>5	—	>5	—
Complex 2	0.021	0.0114–0.039	0.067	0.046–0.095	0.009	0.007–0.013

All experiments were conducted with  $n \geq 3$ , except for <sup>a</sup> ( $n = 1$ ) and <sup>b</sup> ( $n = 2$ ). Three biological repeats were conducted for all experiments.

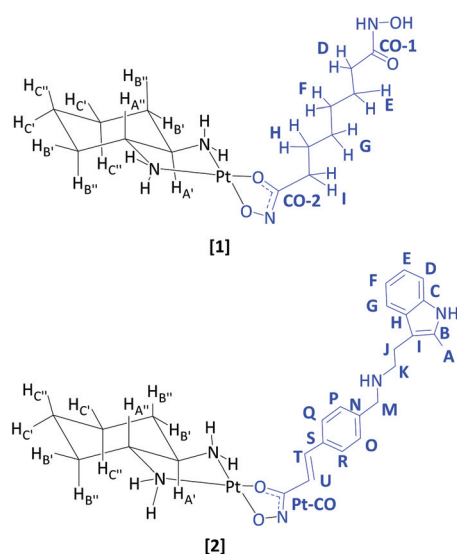


**Fig. 3** Novel platinum(II) complexes: [Pt<sup>II</sup>(*R,R*-DACH)(Sub<sub>H</sub>)] (**1**), [Pt<sup>II</sup>(*R,R*-DACH)(panobinostat-2H)] (**2**).

<sup>195</sup>Pt) and UV-vis spectroscopy. HRMS of [**1** + H]<sup>+</sup> (C<sub>14</sub>H<sub>28</sub>N<sub>4</sub>O<sub>4</sub>PtH: 512.1829 *m/z* found; 512.1821 *m/z* calculated (1.5 ppm error) (Fig. S1†) and HRMS of [**2** + H]<sup>+</sup> (C<sub>27</sub>H<sub>35</sub>N<sub>5</sub>O<sub>2</sub>PtH: 657.2522 *m/z* found; 657.2511 *m/z* calculated (1.7 ppm error) (Fig. S2†) were in good agreement with theoretical values.

<sup>195</sup>Pt NMR spectroscopic resonances were also observed in the expected spectral region; with resonances for complex **1** at −1973 ppm (D<sub>2</sub>O; −1947 ppm in *d*<sub>7</sub>-DMF) and complex **2** at −1918 ppm (DMF-*d*<sub>7</sub>) (Fig. S30†), in a similar region to the resonance reported for oxaliplatin (−1989 ppm, *d*<sub>7</sub>-DMF).<sup>38</sup> The structures of **1** and **2** were both assigned as far as possible from 1D and 2D NMR spectra, and alternative coordination modes were also considered (see ESI†). A change in chemical shifts for the coordinated ligands compared to the free hydroxamic acids were observed by both <sup>1</sup>H NMR and <sup>13</sup>C NMR spectroscopy, with <sup>1</sup>H integral ratios also supporting ligand

complexation. For both **1** and **2**, platinum coordination of the ligand induced inequivalence in the <sup>13</sup>C NMR spectral resonances in the *R,R*-DACH ring, consistent with a reduction in symmetry of the platinum(II) complex, in comparison to oxaliplatin. For complex **1**; small resonances which may correlate to DACH-NH<sub>2</sub> protons were observed in D<sub>2</sub>O at 5.87 ppm and 5.19 ppm (Fig. S11†). Acquiring the <sup>1</sup>H NMR spectra of **1** in DMF-*d*<sub>7</sub> enabled unequivocal visualisation of the four DACH-NH<sub>2</sub> proton environments, which were deshielded compared to oxaliplatin: being observed at 6.38 ppm and 6.34 ppm (H<sub>J</sub>, H<sub>L</sub>), and 5.62 ppm and 5.55 ppm (H<sub>K</sub>, H<sub>M</sub>), and 6.35 ppm and 5.57 ppm in **1** (DMF-*d*<sub>7</sub>, Fig. S12†), in comparison to 6.15 ppm and 5.35 ppm in oxaliplatin (DMF-*d*<sub>7</sub>, Fig. S2†). These resonances showed correlations to one another and to the DACH H<sub>A'</sub> and H<sub>A''</sub> protons (COSY, Fig. S13†). Resonances at higher field (12.56 ppm, 10.68 ppm and 9.08 ppm) all exchanged with the H<sub>2</sub>O resonance at 3.70 ppm. The resonance at 12.56 ppm showed an HMBC correlation to CO-2 (171.6 ppm) and may correspond with solution protonation of the platinum-coordinated hydroxamic acid group; the resonance at 10.68 ppm shows an HMBC correlation to CO-1 (170.7 ppm) and is fairly similar to the hydroxamic acid OH resonance in the free ligand at 10.32 ppm (*d*<sub>6</sub>-DMSO). The inequivalence of H<sub>I</sub> (2.34 ppm) and H<sub>D</sub> (2.07 ppm) is consistent with one end of the SubH ligand binding to the platinum centre to a greater extent than the other end of the ligand. For complex **2**; multiple functional groups are present in panobinostat which could potentially coordinate to the platinum centre including the hydroxamic acid, the alkene (η<sup>2</sup>-coordination), the aliphatic amine and the indole amine. Comparing the <sup>1</sup>H NMR spectrum of **2** to free panobinostat, there was a notable change in resonances assigned to the vinyl protons, which moved from 6.62 ppm to 6.91 ppm (H<sub>U</sub>) and from 7.53 ppm to 7.45 ppm (H<sub>T</sub>). This change could be indicative of either the alkene or hydroxamic acid group coordinating to platinum, however, no platinum satellites were detected in the <sup>13</sup>C NMR spectrum for either C<sub>U</sub> or C<sub>T</sub> (anticipated coupling *ca.* <sup>1</sup>J<sub>PtC</sub> = 153 Hz reported for [PtCl<sub>2</sub>(COD)]),<sup>39</sup> suggesting that a strong interaction between the alkene and platinum is unlikely, and therefore the deshielding is more likely to be due to



coordination of at least part of the hydroxamic acid group. Whilst the  $^1\text{H}$  NMR spectral resonances of the indole ring were relatively unchanged, systematic deshielding was also observed for the resonances around the aliphatic amine of the panobinostat ligand, possibly indicative of an interaction of this amine with the platinum:  $\text{H}_\text{K}$  was shifted from 2.93 ppm to 3.39 ppm,  $\text{H}_\text{J}$  from 2.84 ppm to 3.22 ppm and  $\text{H}_\text{M}$  from 3.86 ppm to 4.50 ppm. The resonances at 6.52 ppm and 5.74 ppm which correspond to DACH amine protons showed weak HMBC correlations to the DACH  $\text{C}_\text{A'}$  and  $\text{C}_\text{A''}$   $^{13}\text{C}$  NMR spectral resonances. In comparison to free panobinostat, two new singlets were also observed for complex 2 at 13.26 ppm and 9.43 ppm, as well as the resonance at 10.90 ppm (possibly a hydroxamic acid OH group), similar to the coordination behaviour observed for complex 1. These new resonances could be NH groups, but are difficult to assign further, the resonance at 9.43 ppm showed no HMBC correlations (the HMBC experiment did not incorporate the 13.26 ppm resonance). If this is the case, it could imply protonation/retention of the hydroxamic acid OH group following platinum coordination (see Fig. S23†).

### Stability of complexes 1 and 2

The solution stability of complexes 1 ( $\text{D}_2\text{O}$ ) and 2 ( $\text{DMF-}d_7$ ) was investigated by  $^1\text{H}$  NMR spectroscopy and HPLC.  $^1\text{H}$  NMR spectroscopy demonstrated that complexes 1 and 2 were unchanged in  $\text{D}_2\text{O}$  and  $\text{DMF-}d_7$  respectively for at least 3 d at 18 °C, with no free hydroxamic acid ligand observed. When the complexes 1 and 2 were analysed by HPLC under either neutral or basic conditions, free ligand (205.15  $m/z$  for  $[\text{SubH} + \text{H}]^+$  and 350.20  $m/z$  for  $[\text{panobinostat} + \text{H}]^+$ ) was observed, suggesting that the hydroxamic ligands are partially labile under HPLC conditions. For both complexes, carboxylic acid derivatives of the hydroxamic acid ligands (suggested to have formed *via* nitrosocarbonyl intermediates<sup>40</sup>) were also detected in the HPLC trace (Fig. S34†); for complex 1,  $[\text{SubH} - \text{NH}] + \text{H}]^+$  (F) was detected at 190.08  $m/z$  (model 190.11  $m/z$ , positive ionisation mode). For complex 2,  $[\text{pano} - \text{NH}] + \text{H}]^+$  (G) was detected at 335.16  $m/z$  (model 333.18  $m/z$ , positive ionisation mode) and the corresponding species  $[\text{pano} - \text{NH}_2]^-$  (H) was detected at 333.12  $m/z$  (model 333.16  $m/z$ , negative ionisation mode) at the same retention time. However, these carboxylate derivatives were also observed during HPLC analysis of the free ligands (SubH and panobinostat) alone.

### Attempted oxidation of 1 and 2 to platinum(IV) complexes

The oxidation of complex 1 (20 mg in 5 ml  $\text{H}_2\text{O}$  and 3 eq.  $\text{H}_2\text{O}_2$ ) at ambient temperature was monitored over a period of 24 h by HPLC; formation of  $[\text{Pt}^{\text{IV}}(\text{R,R-DACH})(\text{Sub})(\text{OH})_2]$  (3) (detected as  $[\text{3} + \text{H}]^+$ ) was confirmed by HRMS ( $\text{C}_{14}\text{H}_{30}\text{N}_4\text{O}_6\text{PtH}$ : 546.1887  $m/z$  found; 546.1886  $m/z$  calculated, 0.18 ppm error) (Fig. S35†), but the reaction did not proceed to completion, despite extended reaction times (48 h). Several aggregation species and fragmentation products of 3 were also observed, supporting the identification of the oxidised product (Fig. S36†). Complex 3 was isolated by mass-directed HPLC as

a pale yellow solid, however, following solvent removal (lyophilisation) 3 readily decomposed, forming a black  $\text{Pt}(0)$  precipitate. Use of more forcing conditions (excess  $\text{H}_2\text{O}_2$ , reaction temperatures of 45 °C, 55 °C or 75 °C) did not improve conversion to 3, as judged by HPLC. Despite repeated attempts to purify and analyse 3 (including isolation of the product by precipitation with diethyl ether from the reaction solution, as an alternative to HPLC purification), the complex was not sufficiently stable to enable further meaningful characterisation.

The attempted oxidation of 2 was also monitored by HPLC: the starting complex 2 (detected as the  $[\text{M} + \text{H}]^+$  ion at 657.25  $m/z$ ) was gradually consumed over a period of 4 h (50 °C, 30 eq.  $\text{H}_2\text{O}_2$ , DMF), but oxidised product  $[\text{Pt}^{\text{IV}}(\text{R,R-DACH})(\text{panobinostat}_{2\text{H}})(\text{OH})_2]$  was not detected under any conditions (anticipated at 691.26  $m/z$ ).

### Compound interaction studies

We conducted brief investigations into the interactions between panobinostat (often administered orally)<sup>41</sup> and carboplatin or oxaliplatin (administered intravenously) in solution, since it is typical for hydroxamic acid HDAC inhibitors (*e.g.* SAHA) and platinum(II) complexes (*e.g.* carboplatin) to be administered on the same day during clinical treatment regimes.<sup>31,32</sup>

Solutions containing oxaliplatin (2 mg in 0.5 mL  $\text{H}_2\text{O}$ ) and panobinostat (2 mg in 0.5 mL DMF) were mixed. The vial became warm and a white precipitate formed within 1 min of mixing. This reactivity was not observed when the panobinostat solution (DMF) was mixed with  $\text{H}_2\text{O}$  only (*i.e.* no oxaliplatin). The solution was filtered to remove the precipitate and the filtrate analysed by HPLC at regular timepoints: complex 2 was only detected (as  $[\text{2} + \text{H}]^+$ , 657.29  $m/z$ ,  $t_\text{R}$  = 5.4 min) at a very low concentration in the filtrate 24 h after mixing. The experiment was repeated at a lower concentration (as above, but with 0.75 mg compound/0.5 mL solvent) resulting in minimal precipitate formation, such that the reaction could be monitored directly by NMR spectroscopy.  $^{195}\text{Pt}$  and  $^1\text{H}$  NMR spectral monitoring showed only oxaliplatin and panobinostat, with no change or evidence of 2 formation for at least 8 days. At 8 days, HPLC analysis of the NMR sample showed presence of 2 (in addition to panobinostat and oxaliplatin) but a simultaneous  $^1\text{H}$  NMR spectrum did not, suggesting that 2 is formed only at low concentrations, below the  $^1\text{H}$  NMR spectroscopic detection limit. To identify the precipitate, the experiment was repeated at higher concentration (as above, but 5 mg compound/0.5 mL solvent) and both solutions were syringe-filtered before mixing. The off-white precipitate (6 mg) was isolated by filtration and dried under vacuum before being re-suspended in  $\text{DMF-}d_7$ .  $^1\text{H}$ ,  $^{195}\text{Pt}$  and  $^{13}\text{C}$  NMR spectra showed a panobinostat-like compound, with no  $^{195}\text{Pt}$  resonances observed over the anticipated  $^{195}\text{Pt}$  spectral range ( $\delta$ : -1204 ppm to -2395 ppm), and crucially no *R,R*-DACH resonances were detected in the  $^1\text{H}$  NMR spectrum. Although at higher chemical shifts (>4 ppm) the  $^1\text{H}$  NMR spectra of panobinostat and the precipitate were identical, a slight shielding





of the aliphatic protons (M, K and J) around the aliphatic amine was observed for the precipitate in comparison to free panobinostat (Fig. S31<sup>†</sup>), possibly indicating a change in the protonation state of the amine group. HPLC analysis of the precipitate was consistent with this, showing predominantly panobinostat (350.06 *m/z*) and the panobinostat fragmentation product (G, Fig. S34,† at 335.05 *m/z*) with small contaminants of oxaliplatin ( $[M + H]^+$  at 398.94 *m/z*) and with no evidence of complex 2. The filtrate did not produce further precipitate on standing. HPLC and NMR spectral analysis of the commercial oxaliplatin sample used confirmed a high level of purity (see ESI<sup>†</sup>). Overall, this suggests that the white precipitate is a panobinostat derivative, rather than a panobinostat-oxaliplatin compound. The mixing was repeated with solutions of carboplatin (2 mg in 0.5 mL H<sub>2</sub>O) and panobinostat (2 mg in 0.5 mL DMF); no precipitate formed, and HPLC analysis showed no observable formation of a carboplatin adduct of panobinostat, monitored over a period of 3 d.

### Biological studies

Complexes 1 and 2 were evaluated *in cellulo* alongside established complexes oxaliplatin, carboplatin, panobinostat and SubH, as well as 1 : 1 mixtures of oxaliplatin with SubH and panobinostat (Table 1 and Fig. S37<sup>†</sup>). Cytotoxicity values for carboplatin<sup>4,6</sup> and panobinostat<sup>6</sup> have previously been reported in DIPG cell lines, but we could find no reports evaluating either oxaliplatin or SubH for DIPG. We used three well-characterised, patient-derived, low passage DIPG cell lines with different mutational statuses in the key driver mutations (H3K27M and ALK2). H<sub>2</sub>O (carboplatin) or DMF (all other compounds) was used for solubilising compounds for cell testing, the toxicity of DMF itself was shown to be negligible at the concentrations used. Cisplatin, carboplatin and oxaliplatin are known to be unstable in DMSO : buffer mixtures, for this reason DMSO was avoided.<sup>42,43</sup> SubH showed no observable cytotoxicity towards the cell lines, and mixtures of SubH and oxaliplatin were less cytotoxic than oxaliplatin alone. Panobinostat was potentially cytotoxic towards all three cell lines, particularly SU-DIPG-IV; consistent with the value of ~0.1 μM reported for a range of DIPG lines.<sup>6</sup>

Mixtures of panobinostat and oxaliplatin were slightly less potent than panobinostat alone. Carboplatin showed no observable toxicity towards the DIPG cell lines at the concentrations evaluated, consistent with reports of IC<sub>50</sub> values >100 μM in seven DIPG lines, including SU-DIPG-IV, which was evaluated here.<sup>6</sup> It is noted however that other glioma cell lines are known to demonstrate sensitivity to carboplatin (*e.g.* cell lines DUB D003: IC<sub>50</sub> 0.047 mg mL<sup>-1</sup>; SF8628 IC<sub>50</sub> 0.026 mg mL<sup>-1</sup> and SF7761 IC<sub>50</sub> 0.0048 mg mL<sup>-1</sup>).<sup>4</sup>

## Discussion

### Synthesis, characterisation and stability of novel platinum complexes

Since several hydroxamic acid-chelated platinum(II) complexes have been previously reported,<sup>44</sup> equatorial hydroxamic acid

chelation was investigated, as an alternative route to complexation. Oxaliplatin was selected as the parent complex, due to encouraging preliminary cytotoxicity data (Table 1). It was envisaged that the platinum(II) complex could act as a “carrier” of the chelated hydroxamic acid – with the potential to improve the solubility in the case of panobinostat – with the hydroxamic acid being released from the platinum(II) complex *in cellulo* in a similar manner to dissociation of the oxalate ligand from oxaliplatin. The platinum(II) complexes of SubH and panobinostat (1 and 2 respectively) were successfully synthesised and characterised, with analytical data consistent with the proposed structures. For previously reported platinum(II) hydroxamic acid complexes, the hydroxamic acid ligand was demonstrated to have rearranged to a hydroximic acid through deprotonation of the nitrogen and delocalisation of the carbonyl double bond in the coordinated complex (Fig. 4, Complex F),<sup>35</sup> and we suggest that this is the most likely coordination geometry in 1 and 2, although alternative binding modes are presented in the ESI.<sup>†</sup> Since the integrity of the released hydroxamic acid was also important for preserving potential HDAC inhibitory activity, this was investigated by HPLC.

Although a small amount of degraded hydroxamic acid (F and G/H) was detected, this was roughly constant with the intensities observed during HPLC analysis of solutions of the free hydroxamic ligands themselves. The majority of the ligand which was released from 1 and 2 was detected as the protonated intact hydroxamic acid – either free SubH or panobinostat – rather than the degraded forms, suggesting that the hydroxamic acid ligands are relatively labile from the complex under HPLC conditions, and that release from 1 and 2 does not result in any appreciable degradation of the hydroxamic acid.

### Attempted oxidation of 1 and 2 to platinum(IV) complexes

Platinum(IV) complexes typically demonstrate greater kinetic inertness towards ligand substitution compared with platinum(II) complexes, due to their octahedral, d<sub>6</sub> configuration.<sup>11</sup> It was envisaged that such a platinum(IV) complex could retain coordination of the hydroxamic acid until the complex was reduced to platinum(II) *in cellulo*.

Previous attempts to oxidise platinum(II) hydroxamate complexes have met with mixed success; attempted oxidation of a platinum(II) pyridinehydroxamate complex resulted in formation of a platinum(IV) complex with axial chlorido, rather than hydroxido ligands, and also resulted in destruction of the hydroxamic acid group to form a carboxylic acid.<sup>45</sup>

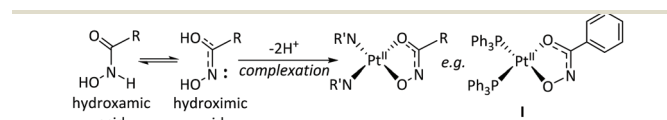


Fig. 4 Previously reported hydroxamic acid complexation modes for Pt(II); complex I: [Pt(sha-H)(PPh<sub>3</sub>)<sub>2</sub>].<sup>35</sup>



Furthermore, hydroxamic acids have been reported to facilitate reduction of platinum(IV) to platinum(II).<sup>46</sup> However, we felt it was of interest to briefly investigate the possibility of accessing platinum(IV) derivatives of **1** and **2**, since there was the possibility that hydroxamic chelation could be stabilised due to the hydroxamic acid favouring harder metal ions (Pt<sup>IV</sup> vs. Pt<sup>II</sup>), and the relative inertness of the d<sub>6</sub>-configuration. Whilst ESI-MS provided evidence that **1** had been successfully oxidised to **3**, this compound was unstable and a purified sample could not be further analysed. No evidence of oxidation of complex **2** was observed.

### Biological investigations

As a mutant histone phenotype is observed in up to 80% of DIPG cases, the use of HDAC inhibitors in combination with other agents is a promising line of investigation for DIPG.<sup>47</sup> We determined that oxaliplatin, complex **2** and panobinostat showed good activity towards SU-DIPG-IV (*HIST1H3B* and *ACVR1-R206H* mutant) and SUDIPG-XXI (*HIST1H3B* and *ACVR1-G328W* mutant) lines. This is encouraging, since oxaliplatin has not previously been identified as a potential treatment for DIPG. There was however, no synergy observed for treatment with both oxaliplatin and panobinostat in a 1 : 1 ratio, under the conditions tested. Furthermore, the cytotoxicity of complex **2** is 3–10 fold lower than that of panobinostat itself. This demonstrates that complexation has impacted on the absolute cytotoxicity of panobinostat. However, this is not necessarily concerning, partly because cell culture is often not the best indicator of the *in vivo* activity of a prodrug, and also because it is too early to comment on the specificity of activity of **2** towards DIPG in comparison to non-cancerous cells. Determining if complexation can reduce the broad spectrum toxicity of panobinostat is planned in subsequent work. All compounds, including the broad-spectrum HDAC inhibitor panobinostat were more effective in the two cell lines with driver mutations than the BIOMEDE 194 (wild type in both driver mutations) cell line. Since oxaliplatin is likely to exert its cytotoxic effect through a different mechanism of action to panobinostat, this suggests a global increase in sensitivity in the cells harbouring driver mutations, but further work is needed to elucidate the precise reasons and mechanisms of cell death. In comparison to oxaliplatin, carboplatin showed only modest cytotoxicity towards the DIPG cell lines under the conditions reported here.<sup>6</sup>

this was insufficiently stable for analysis beyond ESI-MS, decomposing on isolation, and making further development of **3** as an anti-cancer Pt(IV) prodrug unlikely. We were unable to oxidise the panobinostat complex **2** to the corresponding dihydroxido Pt(IV) species.

Complexes **1** and **2** were biologically evaluated in three low-passage patient-derived DIPG cell lines, alongside both established compounds and 1 : 1 mixtures of those compounds. Oxaliplatin showed good activity towards the three DIPG cell lines, whereas carboplatin showed modest cytotoxicity in these lines. To our knowledge, oxaliplatin has not been previously evaluated for DIPG, either *in cellulo* or *in vivo*. Complex **2** showed significantly greater cytotoxicity than oxaliplatin towards all three DIPG cell lines. We observed no obvious synergies *in cellulo* for any of the mixtures of compounds. The unexpected immediate reactivity observed on mixing oxaliplatin and panobinostat solutions *in vitro* formed a precipitate which was determined to be largely panobinostat, with no platinum complexation observed. The same reactivity was not observed between panobinostat and carboplatin. Since **2** does not include the oxalate ligand, the potential for side-effects of peripheral neuropathy are anticipated to be reduced for **2**, in comparison to oxaliplatin. Although complex **2** was moderately less cytotoxic than panobinostat towards all three DIPG cell lines, it exhibited greater aqueous solubility than panobinostat, such that it could potentially be infused by CED at a higher concentration, a key current limitation of panobinostat. Panobinostat is also known to exhibit broad-spectrum toxicity, including towards non-cancerous cells; it is therefore of interest to determine the selectivity of **2**, in comparison to panobinostat. HPLC investigations suggested that panobinostat could be released intact (as a hydroxamic acid) from complex **2**, such that it would be anticipated to retain HDAC inhibitory activity *in cellulo*. Further investigations into the detailed biological effects of oxaliplatin and **2** – including HDAC inhibitory activity for **2** – in a wider panel of patient-derived low-passage DIPG cell lines and (non-cancerous) astrocytes are currently underway.

### Conflicts of interest

There are no conflicts to declare.

### Experimental

For Materials, Methods and Procedures see ESI.†

### Conclusions

Two novel Pt<sup>II</sup> complexes **1** (SubH derivative) and **2** (panobinostat derivative) have been synthesised and characterised. Complex **1** could be oxidised to the platinum(IV) complex **3** but

### Acknowledgements

This work was supported by the Wellcome Trust (201406/Z/16/Z), Cancer Research UK (CR-UK) C5255/A18085, through the CRUK Oxford Centre and the John Fell Fund. We thank Prof. Chris Jones and Prof. Michelle Monje for the DIPG cell lines, Prof. Alex Bullock for assistance with cellular assays and Profs. Stephen Faulkner, Stuart Conway and Akane Kawamura for helpful discussions.



## References

- ONS 2015 Death Registration Summary Tables, England & Wales, Table 2 at: <http://www.ons.gov.uk/peoplepopulationandcommunity/birthsdeathsandmarriages/deaths/datasets/deathregistrationssummarytablesenglandandwalesreferencetables>.
- Q. T. Ostrom, H. Gittleman, J. Xu, C. Kromer, Y. Wolinsky, C. Kruchko and J. S. Barnholtz-Sloan, *Neuro-Oncol.*, 2016, **18**, v1.
- H. S. Gwak and H. J. Park, *Crit. Rev. Oncol. Hematol.*, 2017, **120**, 111.
- C. L. Killick-Cole, W. G. B. Singleton, A. S. Bienemann, D. J. Asby, M. J. Wyatt, L. J. Boulter, N. U. Barua and S. S. Gill, *PLoS One*, 2017, **12**, e0176855.
- N. U. Barua, S. P. Lowis, M. Woolley, S. O'Sullivan, R. Harrison and S. S. Gill, *Acta Neurochir.*, 2013, **155**, 1459.
- C. S. Grasso, Y. Tang, N. Truffaux, N. E. Berlow, L. Liu, M. A. Debily, M. J. Quist, L. E. Davis, E. C. Huang, P. J. Woo, A. Ponnuswami, S. Chen, T. B. Johung, W. Sun, M. Kogiso, Y. Du, L. Qi, Y. Huang, M. Hütt-Cabezas, K. E. Warren, L. Le Dret, P. S. Meltzer, H. Mao, M. Quezado, D. G. Van Vuurden, J. Abraham, M. Fouladi, M. N. Svalina, N. Wang, C. Hawkins, J. Nazarian, M. M. Alonso, E. H. Raabe, E. Hulleman, P. T. Spellman, X. N. Li, C. Keller, R. Pal, J. Grill and M. Monje, *Nat. Med.*, 2015, **21**, 555.
- W. G. B. Singleton, A. S. Bieneman, M. Woolley, D. Johnson, O. Lewis, M. J. Wyatt, S. J. P. Damment, L. J. Boulter, C. L. Killick-Cole, D. J. Asby and S. S. Gill, *J. Neurosurg. Pediatr.*, 2018, 288.
- T. Hennika, G. Hu, N. G. Olaciregui, K. L. Barton, A. Ehteda, A. Chitranjan, C. Chang, A. J. Gifford, M. Tsoli, D. S. Ziegler, A. M. Carcaboso and O. J. Becher, *PLoS One*, 2017, **12**, 1.
- W. G. Singleton, A. M. Collins, A. S. Bienemann, C. L. Killick-Cole, H. R. Haynes, D. J. Asby, C. P. Butts, M. J. Wyatt, N. U. Barua and S. S. Gill, *Int. J. Nanomed.*, 2017, **12**, 1385.
- H. Kommedi, U. Tosi, U. B. Maachani, H. Guo, C. S. Marnell, B. Law, M. M. Souweidane and R. Ting, *ACS Med. Chem. Lett.*, 2018, **9**, 114.
- D. Gibson, *J. Inorg. Biochem.*, 2019, **191**, 77.
- X. Wang, X. Wang, S. Jin, N. Muhammad and Z. Guo, *Chem. Rev.*, 2019, **119**, 1138.
- R. G. Kenny, S. W. Chuah, A. Crawford and C. J. Marmion, *Eur. J. Inorg. Chem.*, 2017, 1596.
- M. Ravera, E. Gabano, M. J. McGlinchey and D. Osella, *Inorg. Chim. Acta*, 2019, **492**, 32.
- E. Petruzzella, J. P. Braude, J. R. Aldrich-Wright, V. Gandin and D. Gibson, *Angew. Chem., Int. Ed.*, 2017, **56**, 11539.
- F. P. Intini, J. Zajac, V. Novohradsky, T. Saltarella, C. Pacifico, V. Brabec, G. Natile and J. Kasparkova, *Inorg. Chem.*, 2017, **56**, 1483.
- F. Yang, N. Zhao, D. Ge and Y. Chen, *RSC Adv.*, 2019, **9**, 19571.
- R. Codd, *Coord. Chem. Rev.*, 2008, **252**, 1387.
- P. Bose, Y. Dai and S. Grant, *Pharmacol. Ther.*, 2014, **143**, 323.
- T. Eckschlager, J. Plch, M. Stiborova and J. Hrabeta, *Int. J. Mol. Sci.*, 2017, **18**, 1.
- D. Wang and S. J. Lippard, *Nat. Rev. Drug Discovery*, 2005, **4**, 307.
- P. M. Bruno, Y. Liu, G. Y. Park, J. Murai, C. E. Koch, T. J. Eisen, J. R. Pritchard, Y. Pommier, S. J. Lippard and M. T. Hemann, *Nat. Med.*, 2017, **23**, 461.
- N. B. Roberts, A. Alqazzaz, J. R. Hwang, X. Qi, A. D. Keegan, A. J. Kim, J. A. Winkles and G. F. Woodworth, *J. Neurooncol.*, 2018, **140**, 497.
- R. Oun, Y. E. Moussa and N. J. Wheate, *Dalton Trans.*, 2018, **47**, 6645.
- D. Griffith, M. P. Morgan and C. J. Marmion, *Chem. Commun.*, 2009, 6735.
- V. Brabec, D. M. Griffith, A. Kisova, H. Kosthunova, L. Zerzankova, C. J. Marmion and J. Kasparkova, *Mol. Pharm.*, 2012, **9**, 1990.
- E. Gabano, M. Ravera and D. Osella, *Dalton Trans.*, 2014, **43**, 9813.
- J. Yang, X. Sun, W. Mao, M. Sui, J. Tang and Y. Shen, *Mol. Pharm.*, 2012, **9**, 2793.
- M. Alessio, I. Zanellato, I. Bonarrigo, E. Gabano, M. Ravera and D. Osella, *J. Inorg. Biochem.*, 2013, **129**, 52.
- H. Kosthunova, E. Petruzzella, D. Gibson, J. Kasparkova and V. Brabec, *Chem. – Eur. J.*, 2019, **25**, 5235.
- S. S. Ramalingam, M. L. Maitland, P. Frankel, A. E. Argiris, M. Koczywas, B. Gitlitz, S. Thomas, I. Espinoza-Delgado, E. E. Vokes, D. R. Gandara and C. P. Belani, *J. Clin. Oncol.*, 2010, **28**, 56.
- S. S. Ramalingam, R. A. Parise, R. K. Ramanathan, T. F. Lagattuta, L. A. Musguire, R. G. Stoller, D. M. Potter, A. E. Argiris, J. A. Zwiebel, M. J. Egorin and C. P. Belani, *Clin. Cancer Res.*, 2007, **13**, 3605.
- H. V. K. Diyabalanage, M. L. Granda and J. M. Hooker, *Cancer Lett.*, 2013, **329**, 1.
- B. Liao, Y. Zhang, Q. Sun and P. Jiang, *Cancer Med.*, 2018, **7**, 196.
- M. D. Hall, T. W. Failes, D. E. Hibbs and T. W. Hambley, *Inorg. Chem.*, 2002, **41**, 1223.
- D. Griffith, A. Bergamo, S. Pin, M. Vadori, H. Müller-Bunz, G. Sava and C. J. Marmion, *Polyhedron*, 2007, **26**, 4697.
- S. Kemp, N. J. Wheate, D. P. Buck, M. Nikac, J. G. Collins and J. R. Aldrich-Wright, *J. Inorg. Biochem.*, 2007, **101**, 1049.
- A. C. Tsipis and I. N. Karapetsas, *Dalton Trans.*, 2014, **43**, 5409.
- M. Enders, B. Görling, A. B. Braun, J. E. Seltenreich, L. F. Reichenbach, K. Rissanen, M. Nieger, B. Luy, U. Schepers and S. Bräse, *Organometallics*, 2014, **33**, 4027.
- S. Nourian, R. P. Lesko, D. A. Guthrie and J. P. Toscano, *Tetrahedron*, 2016, **72**, 6037.
- S. F. Jones, J. R. Infante, D. S. Thompson, A. Mohyuddin, J. C. Bendell, D. A. Yardley and H. A. Burris, *Cancer Chemother. Pharmacol.*, 2012, **70**, 471.



- 42 M. D. Hall, K. A. Telma, K. E. Chang, T. D. Lee, J. P. Madigan, J. R. Lloyd, I. S. Goldlust, J. D. Hoeschele and M. M. Gottesman, *Cancer Res.*, 2014, **74**, 3913.
- 43 H. P. Varbanov, D. Ortiz, D. Höfer, L. Menin, M. Galanski, B. K. Keppler and P. J. Dyson, *Dalton Trans.*, 2017, **46**, 8929.
- 44 T. W. Failes, M. D. Hall and T. W. Hambley, *Dalton Trans.*, 2003, **2**, 1596.
- 45 D. Griffith, K. Lyssenko, P. Jensen, P. E. Kruger and C. J. Marmion, *Dalton Trans.*, 2005, 956.
- 46 D. Griffith, A. Chopra, H. Müller-Bunz and C. J. Marmion, *Dalton Trans.*, 2008, **2**, 6933.
- 47 A. Mackay, A. Burford, D. Carvalho, E. Izquierdo, J. Fazal-Salom, K. R. Taylor, L. Bjerke, M. Clarke, M. Vinci, M. Nandhabalan, S. Temelso, S. Popov, V. Molinari, P. Raman, A. J. Waanders, H. J. Han, S. Gupta, L. Marshall, S. Zacharoulis, S. Vaidya, H. C. Mandeville, L. R. Bridges, A. J. Martin, S. Al-Sarraj, C. Chandler, H.-K. Ng, X. Li, K. Mu, S. Trabelsi, D. H.-B. Brahim, A. N. Kisljakov, D. M. Konovalov, A. S. Moore, A. M. Carcaboso, M. Sunol, C. de Torres, O. Cruz, J. Mora, L. I. Shats, J. N. Stavale, L. T. Bidinotto, R. M. Reis, N. Entz-Werle, M. Farrell, J. Cryan, D. Crimmins, J. Caird, J. Pears, M. Monje, M.-A. Debily, D. Castel, J. Grill, C. Hawkins, H. Nikbakht, N. Jabado, S. J. Baker, S. M. Pfister, D. T. W. Jones, M. Fouladi, A. O. von Bueren, M. Baudis, A. Resnick and C. Jones, *Cancer Cell*, 2017, **32**, 520.

